International Journal of Pharmaceutics 403 (2011) 29–36

Contents lists available at ScienceDirect

International Journal of Pharmaceutics

journal homepage: www.elsevier.com/locate/ijpharm

Thermal analysis: A further step in characterizing solid forms obtained by screening crystallization of an API

Thibaud Detoisien[a], Marine Arnoux[a], Pascal Taulelle[c], Didier Colson[b], Jean Paul Klein[b], Stéphane Veesler[a,*]

[a] Centre Interdisciplinaire de Nanosciences de Marseille, CNRS, Aix-Marseille Université, CINaM-UPR3118, Campus de Luminy, Case 913, 13288 Marseille Cedex, France
[b] LAGEP, Laboratoire d'Automatique et de Génie des Procédés, UMR 5007, 43 boulevard du 11 novembre, BP 2077, 69622 Villeurbanne Cedex, France
[c] Oril Industrie, Laboratoires Servier, 13 rue Auguste Desgenétais, 76210 Bolbec, France

ARTICLE INFO

Article history:
Received 12 July 2010
Received in revised form 7 October 2010
Accepted 9 October 2010
Available online 15 October 2010

Keywords:
Crystallization
Polymorphism
Thermal analysis

ABSTRACT

Phase and habit selection is a very important step in the early stages of pharmaceutical development of new APIs. In this paper, we show how observation, diffraction and thermal analysis are complementary methods of solid habit and phase characterization. At the end of phase screening of an API several habits and phases can be discriminated by microscopy, XRPD or Raman spectroscopy. Using thermal methods here allows us to separate the 12 phases discriminated by XRPD into: anhydrous, monohydrate, organic monosolvate and heterosolvate phases.

1. Introduction

When a new API is launched on the market it is essential to have a thorough knowledge of its differing solid phases and to respect the Good Manufacturing Practice Guide for Active Pharmaceutical Ingredients (http://www.ich.org Q7). Recent history in the pharmaceutical industry (Dunitz and Bernstein, 1995) has shown that the emergence of a new phase can seriously compromise the intended process and potentially the patient's life. Chemburkar, of Abbott laboratories, who dealt with the Ritonavir case in the nineties, drew the following conclusion: "Dealing with Polymorphism is Potentially Precarious Practice and the Proper way to Play this game is with Patience and Perseverance" (Chemburkar et al., 2000). It is for this reason that we proposed, in a previous paper, a useful methodology for rapid screening of crystallization conditions and phases in the pharmaceutical industry (Detoisien et al., 2009) for early stages of pharmaceutical development of new APIs. By permitting rapid and complete screening of crystallization medium and temperature for API crystallization, the method allows us to select from the chemical compositions tested those that generate the best crystalline phase with the optimum crystal habit for down-stream processes, storage and handling. 45 media of crystallization (Table 1), in 1 mL vials, were tested in a temperature range of 20–60 °C. 19 solubility curves were estimated, different crystal habits and phases were obtained with less than 5 g of API in 4 weeks generating more than 11.000 pictures using a multiwell set-up (ANACRISMAT, France) coupled with video-microscopy and XRPD. 12 phases were discriminated. Unfortunately, we were not able to determine whether these phases are polymorphs, hydrates or solvates.

The objective of this work is to complement the solid state characterization of the powder samples resulting from this screening we use differential scanning calorimetry (DSC) and thermogravimetry (TGA) (Giron, 1995) in order to determine the nature of the phases crystallized. We reveal how observation, diffraction and thermal analysis are complementary methods for both solid habit and phase characterization.

2. Materials and methods

2.1. Materials

The API (398 g/mol), a hydrochlorate, was supplied as a crystalline powder, denoted phase A, by Oril Industrie and used as received, solvents are of analytical grade. Crystals were observed by optical microscope (Nikon Eclipse TE2000-U) and by scanning electron microscope (SEM) JEOL 6320F. Solid phases were first characterized by X-ray diffraction (XRPD) INEL CPE 120. Thermal analyses were performed with a DSC: Mettler-Toledo DSC1 equipped with a high-sensitivity HSS7 sensor and an Intracooler

* Corresponding author. Tel.: +33 6 6292 2866; fax: +33 4 9141 8916.
E-mail address: veesler@cinam.univ-mrs.fr (S. Veesler).

0378-5173/$ – see front matter © 2010 Elsevier B.V. All rights reserved.
doi:10.1016/j.ijpharm.2010.10.016

Table 1
List of pure and mixed solvents used for screening.

Compound
Water
Ethanol, 2-propanol, methanol, butanol, pentanol, acetone, methyl isobutyl ketone (MIBK)
Hexane, heptane, cyclohexane, methylcyclohexane, toluene, xylene
Ethyl acetate, butyl acetate
Diethyl ether, isopropyl ether, petroleum ether, methyl tert-butyl ether (MTBE), dimethoxyethane (Glyme), triethylene glycol dimethyl ether (Triglyme), 1,4-dioxan
1,2-Dichloroethane, dichloromethane, chloroform, chlorobenzene
Acetonitrile, dimethyl sulfoxide (DMSO), N,N-dimethylformamide (DMF), tetrahydrofuran (THF), N,N-dimethylacetamide (DMAC)
Compound mixed with water in a ratio 50/50%w
Ethanol, methanol, acetone
Hexane, toluene
Ethyl acetate
Isopropyl ether
Dichloromethane, chloroform
Acetonitrile, DMF, THF, DMA

cooling from −100 °C to 450 °C. TGA measurements were performed with a PerkinElmer TGQ4000. Additional melting point measurements were performed in capillaries was done with an electrothermal digital melting point IA9100. The chemical properties of the API cannot be released for reasons of confidentiality.

Table 2
Summary of crystal forms of the API, discriminated by XRPD crystallized from different media.

Phases	Medium
Phase A	Ethanol, 2-propanol, methanol, butanol, hexane[a], heptane[a], cyclohexane[a], methylcyclohexane[a], toluene[a], xylene[a], butyl acetate[a], diethyl ether[a], isopropyl ether[a], MTBE[a], glyme[a],1,4-dioxan[a], chlorobenzene[a], water/ethanol, water/methanol
Phase B	Water
Phase C	Pentanol, triglyme
Phase D	Acetonitrile
Phase E	1,2-Dichloroethane, dichloromethane
Phase F	Chloroform
Phase G	DMF, water/DMF
Phase H	THF
Phase I	Water/acetonitrile, water/THF
Phase J	Water/acetone α
Phase K	Water/DMAC
Phase L	Water/acetone β

[a] Very low solubility in this solvent, lower than 5 mg/mL. As a result, the solid phase A is not dissolved.

2.2. Experimental set-up and procedure

40 μL aluminum pans were used for all DSC measurements. All pans were punctured at the top to facilitate the release of organic

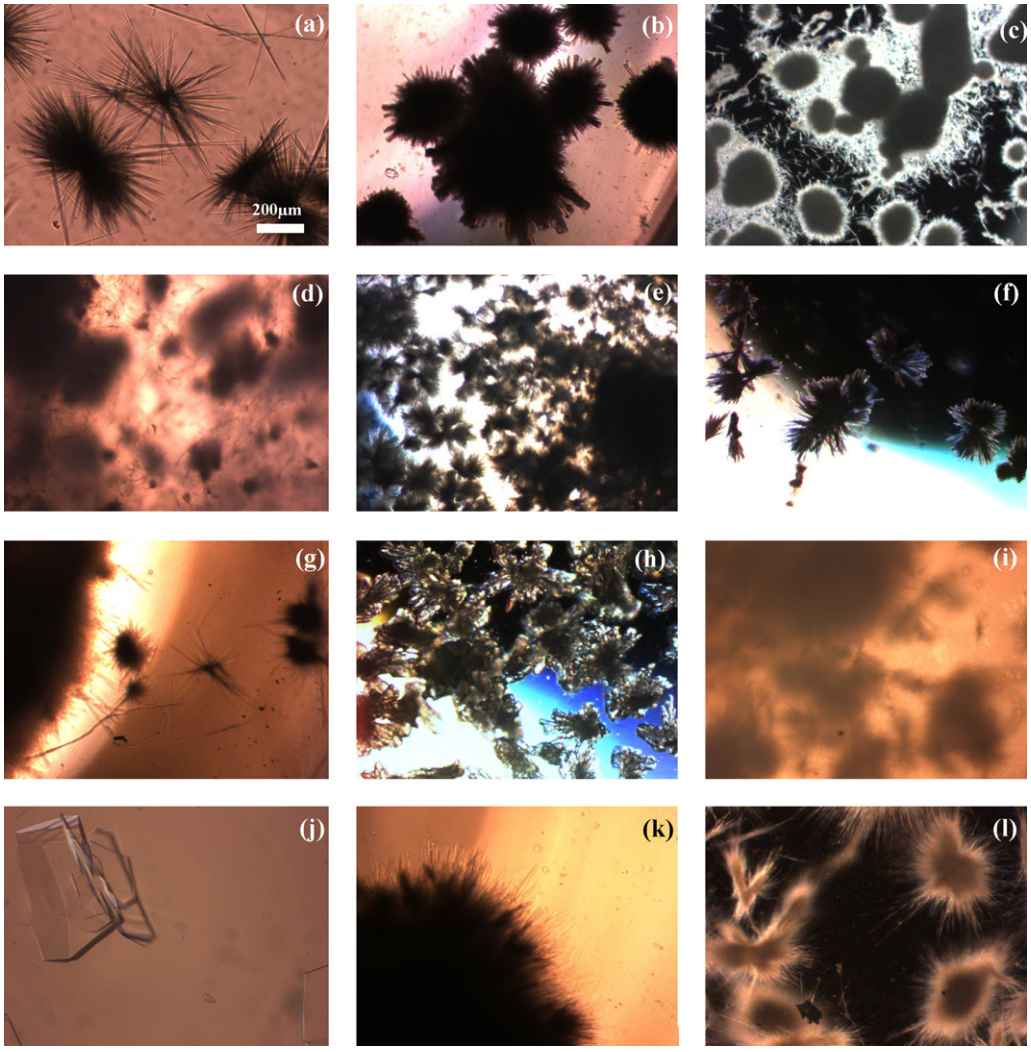

Fig. 1. Summary of crystal forms of the API, forms A to L: (a) to (l). All the optical micrographs are at the same magnification.

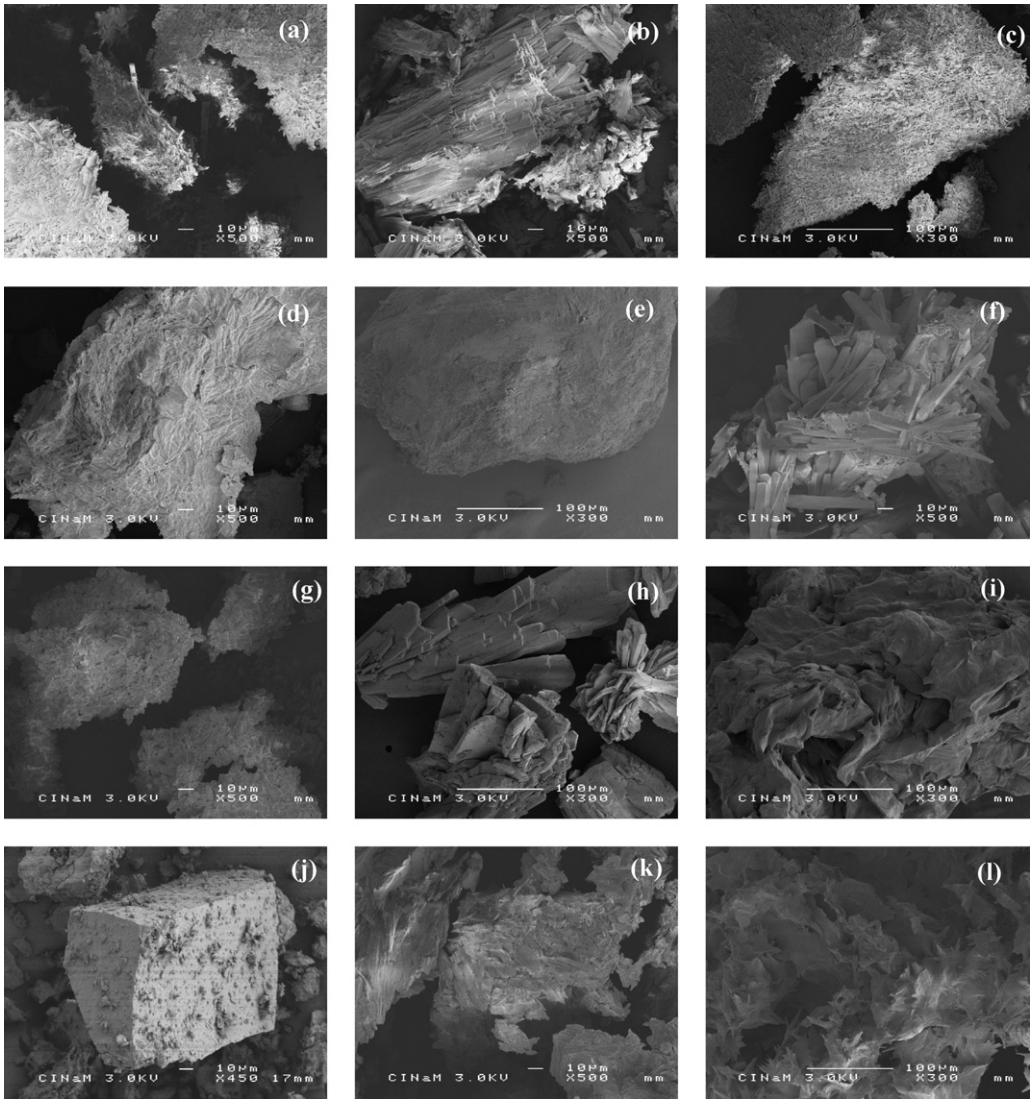

Fig. 2. Summary of crystal forms of the API, SEM micrographs of forms A to L: (a) to (l).

byproducts and residual solvent vapors in order to avoid build-ups of pressure in the pan that would alter the data. Samples were heated from 25 °C to 250 °C at 10 °C min^{-1}. At the end of the experiment, the DSC capsules were opened to observe the materials: either a solid powder, a carbonized powder or a melt. When fusion was not observed, i.e. in the absence of an endothermic peak on the thermogram, measurement was repeated at higher temperature, 300 °C and, if necessary, 350 °C. A maximum of 4 mg is required for a typical DSC measurement under our conditions. When the crystallization screening did not yield sufficient materials for thermal analysis, we duplicated the experiment with the multiwell set-up and checked by XRPD whether we had obtained an identical phase.

For TGA measurements, we heated from 40 °C to 600 °C to ensure pyrolysis of the organic products in the ceramic crucible.

3. Results and discussion

Table 2 summarizes the different crystallization media leading to 12 different phases characterized by XRPD. Optical and scanning electron microscopy (SEM) micrographs of these phases are presented in Figs. 1 and 2, respectively. Before characterizing the nature of the 12 phases crystallized during the solvent screening, we performed a thorough analysis of phase A of the API. Figs. 3 and 6a present DSC and TGA analyses of phase A. The first wide endotherm ($-94.95\,J\,g^{-1}$) between 50 and 120 °C for phase A in Fig. 3 corresponds to the loss of 4.2% weight of water = 94.95/2257, with $2257\,J\,g^{-1}$ the vaporization enthalpy of 1 g of water under atmospheric pressure monitoring (ΔH_V^{Patm}) assuming vaporization enthalpy of water from crystal equal to vaporization enthalpy of water. If phase A was a monohydrate this loss would represent 18/(398 + 18) = 4.3%, with 18 and 398 g mol^{-1} molecular weights of water and API respectively. The width of the endotherm may be due either to kinetic effects from the heating rate of 10 °C min^{-1}, and/or to structural effects (discussion of these points are beyond the scope of this paper). This qualitative estimation, of water loss, is confirmed by TGA under which a loss of 5.6% is observed (Fig. 6a).

Fig. 6a shows that, here again, the weight loss (of water) is observed between 50 and 110 °C.

We conclude that phase A is a monohydrate.

3.1. DSC

Of the twelve phases analyzed with DSC and DRX (Figs. 3–5), only phase E was not melted after heating at 250 °C and was therefore reanalyzed by heating to 300 °C (Fig. 3a). DSC data are

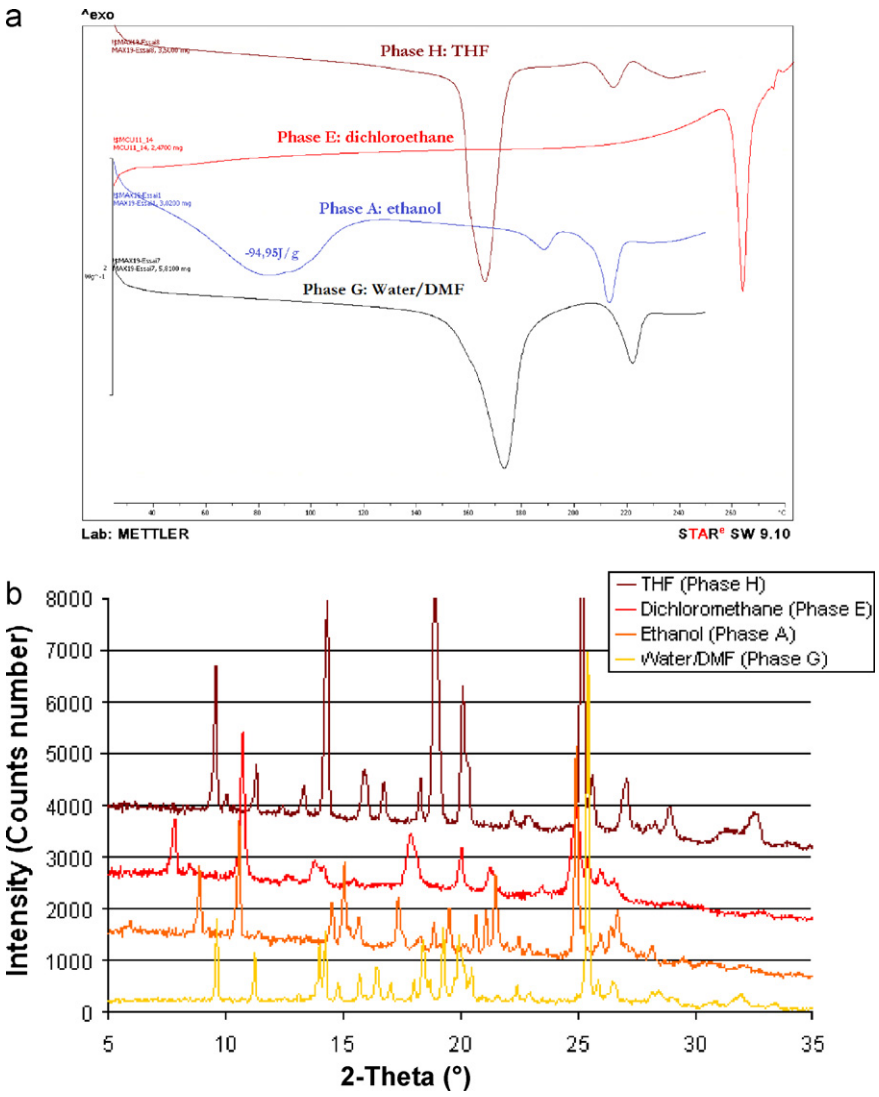

Fig. 3. DSC (a) and XRPD (b) of A, E, G and H phases.

summarized in Table 3 and presented in Figs 3a, 4a and 5a. There are up to three endotherms per DSC thermogram; from these analyses phases can be classified into two categories:

- Category (1): only a narrow endotherm shape and no endotherm at $T < 100\,^{\circ}C$: phases D, E, G, H and K.
- Category (2): a wide endotherm shape starting at $T < 100\,^{\circ}C$: phases A, B, C, F, I, J and L.

For category (1), only phases D and E (Figs. 3a and 5a) present a single endotherm, representing their respective melting points: 225.8 °C and 260.3 °C, therefore there was no solvent loss. In addition, phases G, H and K (Figs. 3 and 4) present two endotherms, well above 100 °C. G and K phases present their first endotherm around the boiling point of the solvent in which they were crystallized: phase G in water/DMF, T_b DMF = 153 °C, endotherm at 158.0 °C and phase K in water/DMAC, T_b DMAC = 164 °C, endotherm at 161.2 °C. Phase H presents its first endotherm at 156.9 °C far from the THF solvent (of crystallization) boiling point (T_b = 66 °C). The second endotherm for all three samples represents the melting of the resulting desolvated phase. These three phases, G, H and K, should be solvates, as later confirmed by a quantitative analysis by TGA, presented hereunder.

In category (2), phase A was clearly identified as a monohydrate.

Phases A, B, C, F, J present a second set of two endotherms at $T > 100\,^{\circ}C$ (Figs. 3a, 4a and 5a). While it is highly probable that the first endotherm at $T < 100\,^{\circ}C$ is representative of a stoichiometric quantity of water molecules in the solid structure, for crystallization conditions corresponding to anhydrous solvent, the water comes from dissolution of phase A. The second endotherm should be representative of the release of other solvent molecules and the third should represent the melting of the desolvated phase as later confirmed by TGA presented hereunder. This assay did not identify the phases as hydrates, mixed solvates or heterosolvates so TGA was used as described hereunder. It is not clear why we did not observe exotherms between endotherms, which would have indicated a solid/solid transformation.

Phases I and L present very similar DSC curves with a wide endotherm of ~27 J g^{-1} between 50 °C and 140 °C and a ~40 J g^{-1} endotherm at 202–203 °C (Figs. 4a and 5a). However, XRPD analysis showed two different diffractograms (Figs. 4b and 5b). Given the crystallization medium composition, phases I and L are probably hydrates.

DSC measurements clearly increase our knowledge of the different phases crystallized after a solvent screening but quantifying all endotherms via hypothetical release enthalpies of

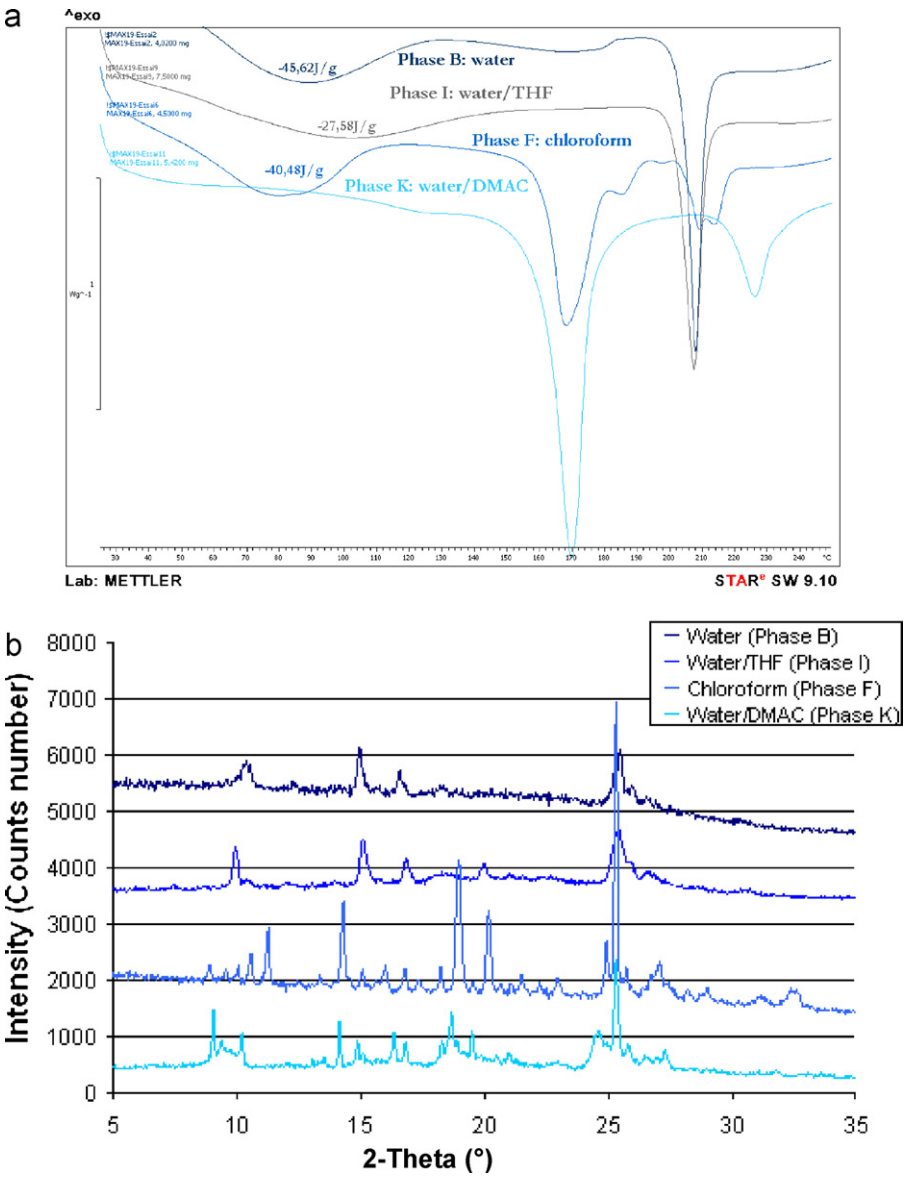

Fig. 4. DSC (a) and XRPD (b) of B, I, F and K phases.

solvent molecules is risky. Complementary TGA measurements are required to obtain quantitative data on the phase compositions.

3.2. TGA

Fig. 6 gives TGA results showing weight changes during heating; heat flow is also plotted but with less precision than in a DSC experiment. Weight loss is characterized by clear decrease in the curve. This quantitative information leads to strong hypotheses on the elements released from the solid structure under heating. Results are summarized in Table 4.

Category (1): phases D, E, G, H and K. Phases D and E did not lose weight before chemical degradation confirming DSC results; these phases are not solvates but true polymorphs. Phase H loses 15.0% of its weight before 166 °C (Fig. 6b), which matches the first DSC endotherm at 156.9 °C (Table 3 and Fig. 3a). The weight of one molecule of solvent in a 1:1 API:THF solvate represents 15.25% weight. TGA confirms the hypothesis of a solvate phase from DSC and specifies its nature and stoichiometry.

Phases G and K present two clear losses, one before 100 °C and the second beginning at 174 °C and 173 °C, respectively. Surprisingly, the first loss, before 100 °C does not appear on DSC. The second loss beginning at 174 °C and 173 °C for G and K, respectively, matches the first DSC endotherm observed at 158.1 °C and 161.2 °C (Table 3 and Figs. 3a and 4a). We cannot explain the differences between DSC and TGA records; we therefore propose a solvate with 1 molecule of DMF and DMAC for G and K, respectively, in agreement with the weight loss at 174 °C and 173 °C observed with TGA.

Category (2): phases A, B, C, F, I, J and L. Phases A, B and C show a single clear loss of ~5.6% before 100 °C (Fig. 6a). With no other weight loss before fusion, these three phases are identified as monohydrates. Note that there is no weight loss associated with the second endothermic peak on the DSC (Figs. 3a and 6a).

Phases F and J present two clear losses of weight, representative of the loss of water and another solvent, respectively chloroform and acetone: they are therefore heterosolvates. These results fully match the DSC results. We propose the following stoichiometries for phase F 1:0.5 H_2O:0.75 chloroform (1.8% of H_2O and 18.0% of chloroform) and phase J 1:0.5 H_2O:0.5 acetone (1.9% of H_2O and 6.9% of acetone).

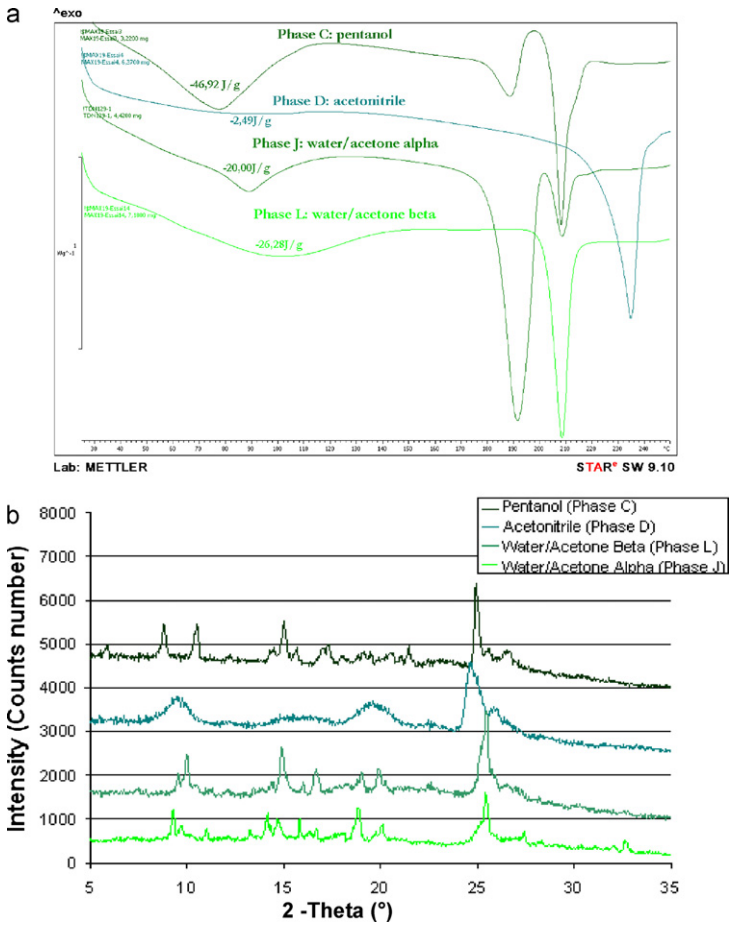

Fig. 5. DSC (a) and XRPD (b) of C, D, L and J phases.

Table 3
Summary of DSC results for the 12 different phases characterized by XRPD.

Phase solvent of crystallization	Solvent data T_b/°C ΔH_V^{Patm}/J g^{-1} Solvent Mw$_i$	Endotherm starting at T < 100 °C Enthalpy/J g^{-1} T-range/°C	Enthalpy/J g^{-1} T/°C		
Phase A Ethanol	78, −855 46 g mol^{-1}	−94.95 50–120	−6.77 180.1	−21.50 208.4	–
Phase B Water	100, −2257 18 g mol^{-1}	−45.62 50–120	−4.92 143.3	−37.89 203.9	–
Phase C Pentanol	138, −647 88 g mol^{-1}	−45.92 30–120	−14.71 179.5	−33.37 204.1	–
Phase D Acetonitrile	82, −810 41 g mol^{-1}	–	–	–	−58.48 225.8
Phase E Dichloroethane	84, −289 99 g mol^{-1}	–	–	–	−43.76 260.3
Phase F Chloroform	62, −247 119 g mol^{-1}	−40.49 40–115	−58.97 161.1	−16.04 204.3	–
Phase G Water/DMF	153, −639 73 g mol^{-1}	–	−133.08 158.1	–	−19.84 215.2
Phase H THF	66, −442 72 g mol^{-1}	–	−119.02 156.9	−9.42 207.8	–
Phase I Water/THF	–	−27.58 50–140	–	−39.75 201.7	–
Phase J Water/acetone α	56, −532 60 g mol^{-1}	−20.00 70–120	−93.85 182.06	−9.45 203.6	–
Phase K Water/DMAC	164, −582 87 g mol^{-1}	–	−90.92 161.2	–	−21.22 218.1
Phase L Water/acetone β	–	−26.28 50–140	–	−40.59 202.3	–

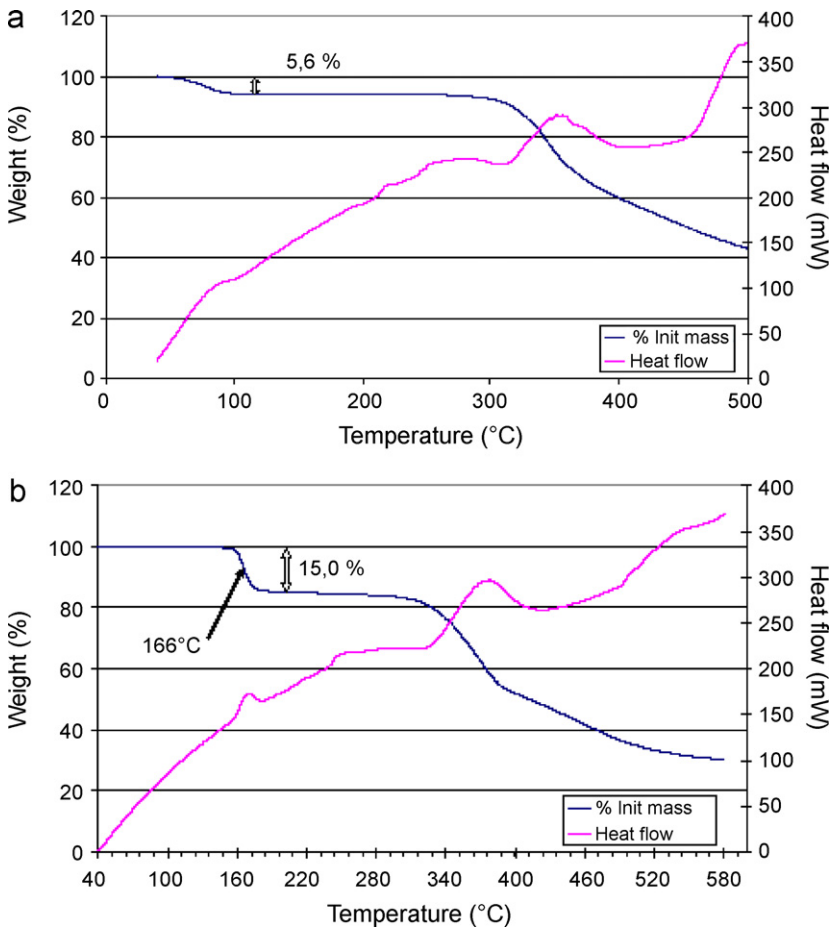

Fig. 6. TGA of phases A (a) and H (b).

Table 4
ATG results for all solid phases discriminated by XRPD.

Phase	Weight loss before chemical degradation	API phase type
Phase A Ethanol	Net loss of 5.6% before 100 °C	Mono hydrate
Phase B Water	Net loss of 5.1% before 100 °C	Mono hydrate
Phase C Pentanol	Net loss of 5.2% before 100 °C	Mono hydrate
Phase D Acetonitrile	Small loss of ~1% until degradation	Anhydrous
Phase E Dichloroethane	No loss before degradation	Anhydrous
Phase F Chloroform	Net loss of 2.5% before 100 °C Net loss of 16.8% beginning at 152 °C => Matches the 1st endotherm	Heterosolvate (1:0.5 H_2O:0.75 chloroform)
Phase G Water/DMF	Net loss of 15.5% before 100 °C Net loss of 13.3% beginning at 154.5 °C => Matches the 1st endotherm	DMF–solvate (1:1)
Phase H THF	Net loss of 15.0% beginning at 151.2 °C => Matches the 1st endotherm	THF–solvate (1:1)
Phase I Water/THF	Loss of 4.8%before 120 °C	Mono hydrate
Phase J Water/acetone α	Net loss of 2.4% before 100 °C Net loss of 6.3% beginning at 171.7 °C => Matches the 1st endotherm	Heterosolvate (1:0.5 H_2O:0.5 acetone)
Phase K Water/DMAC	Net loss of 4.3% before 100 °C Net loss of 17.1% beginning at 150.4 °C => Matches the 1st endotherm	DMAC–solvate (1:1)
Phase L Water/acetone β	Loss of 4.9% before 120 °C	Mono hydrate

Phases I and L lose respectively 4.8% and 4.9% before 100 °C, TGA confirms the hypothesis of hydrate phases formed as a result of DSC measurements. However, the estimated stoichiometries from the enthalpy of vaporization are, for phases I and L, underestimated: from 1 API:0.25 water with DSC to 1:1 with TGA.

To summarize, from DSC and TGA experiments it was possible to separate the 12 phases (previously identified by DRX) into two categories. Category (1): phases D, E, G, H and K: DSC thermograms presenting only a narrow endotherm shape and no endotherm at $T < 100$ °C corresponding to anhydrous phases, two polymorphs D and E and three organic solvates: G, H and K. Category (2) a wide endotherm shape starting at $T < 100$ °C.: phases A, B, C, F, I, J and L all being hydrates. Five are monohydrates A, B, C, I, L and 2 are heterosolvates: F with water and chloroform, and J with water and acetone.

4. Conclusion

Phase and habit selection is a very important step in early stages of pharmaceutical development of new APIs. To allow for downstream processes, storage and handling, it is essential to maintain tight control over physical properties. Moreover, the selection of a solid phase to be given to patients can be envisaged solely if the content of the solvent can be evaluated and monitored to a concentration limit fixed by ICH (http://www.ich.org Q3C(R4)). Thus, it is vital to determine whether the phase crystallized is an asolvate or a solvate, and its composition.

Here, we show how observation, diffraction and thermal analysis are complementary methods of solid habit and phase characterization. At the end of phase screening of an API several habits and phases can be discriminated by microscopy and XRPD (Detoisien et al., 2009) or Raman spectroscopy (Peterson et al., 2002). Using these thermal methods here allows us to separate the 12 phases discriminated by XRPD into: two anhydrous phases, five monohydrates, three organic monosolvates and two heterosolvates with water.

Acknowledgements

We thank Mettler-Toledo, Inc., for the DSC instrument (Mettler-Toledo AG; *Mettler Toledo Academia News*, 2008, 4), and Drs G. Canard and P. Vanloot (IUT, Marseille universities) for the TGA instrument. We thank T. bactivelane (CINaM) and M. Audiffren (Anacrismat) for their help in the development of the multiwell set-up. We thank Servier group for financial support and M. Sweetko for English revision.

References

Chemburkar, S.R., Bauer, J., Deming, K., Spiwek, H., Patel, K., Morris, J., Henry, R., Spanton, S., Dziki, W., Porter, W., Quick, J., Bauer, P., Donaubauer, J., Narayanan, B.A., Soldani, M., Riley, D., Mcfarland, K., 2000. Dealing with the impact of ritonavir polymorphs on the late stages of bulk drug process development. Org. Process Res. Dev. 4, 413–417.

Detoisien, T., Forite, M., Taulelle, P., Teston, J., Colson, D., Klein, J.P., Veesler, S., 2009. A rapid method for screening crystallization conditions and phases of an active pharmaceutical ingredient. Org. Process Res. Dev. 13, 1338–1342.

Dunitz, J.D., Bernstein, J., 1995. Disappearing polymorphs. Acc. Chem. Res. 28, 193–200.

Giron, D., 1995. Thermal analysis and calorimetric methods in the characterisation of polymorphs and solvates. Thermochim. Acta 248, 1–59.

Peterson, M.L., Morissette, S.L., Mcnulty, C., Goldsweig, A., Shaw, P., Lequesne, M., Monagle, J., Encina, N., Marchionna, J., Johnson, A., Gonzalez-Zugasti, J., Lemmo, A.V., Ellis, S.J., Cima, M.J., Almarsson, O., 2002. Iterative high-throughput polymorphism studies on acetaminophen and an experimentally derived structure for form III. J. Am. Chem. Soc. 124, 10958–10959.